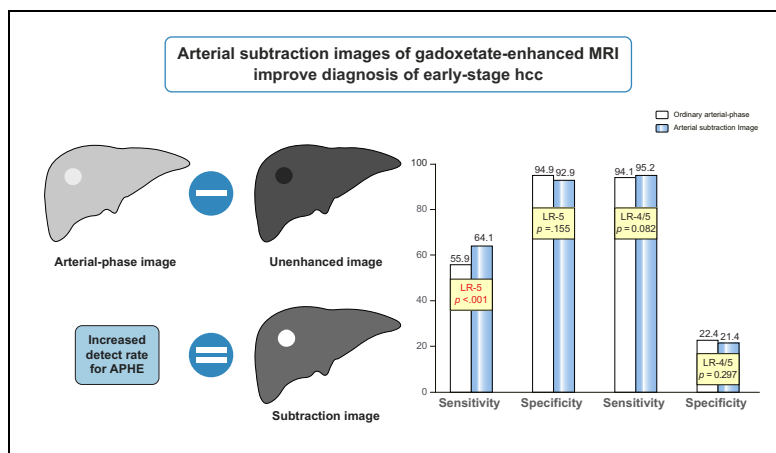


Arterial subtraction images of gadoxetate-enhanced MRI improve diagnosis of early-stage hepatocellular carcinoma

Graphical abstract



Highlights

- Arterial subtraction images show more arterial hyperenhancement than arterial images.
- Arterial subtraction images significantly increase sensitivity for the diagnosis of HCC.
- Arterial subtraction images do not significantly decrease specificity.
- Arterial subtraction images can be useful for diagnosing early-stage HCC.

Authors

Dong Hwan Kim, Sang Hyun Choi, Jae Ho Byun, ..., Hyung Jin Won, Yong Moon Shin, Pyo-Nyun Kim

Correspondence

jhbyun@amc.seoul.kr (J.H. Byun)

Lay summary

Gadoxetate disodium-enhanced magnetic resonance imaging is an imaging technique with a high sensitivity for the diagnosis of hepatocellular carcinoma. However, arterial-phase images may be unsatisfactory because of weak arterial enhancement. We found that using arterial subtraction images led to clinically meaningful improvements in the diagnosis of early-stage hepatocellular carcinoma.



Arterial subtraction images of gadoxetate-enhanced MRI improve diagnosis of early-stage hepatocellular carcinoma

Dong Hwan Kim^{1,†}, Sang Hyun Choi^{1,†}, Jae Ho Byun^{1,*}, Ji Hun Kang¹, Young-Suk Lim², So Jung Lee¹, So Yeon Kim¹, Hyung Jin Won¹, Yong Moon Shin¹, Pyo-Nyun Kim¹

¹Department of Radiology and Research Institute of Radiology, University of Ulsan College of Medicine, Asan Medical Center, 88 Olympic-Ro 43-Gil, Songpa-Gu, Seoul 05505, Republic of Korea; ²Department of Gastroenterology, Liver Center, University of Ulsan College of Medicine, Asan Medical Center, 88 Olympic-Ro 43-Gil, Songpa-Gu, Seoul 05505, Republic of Korea

Abstract

Background & Aims: Although gadoxetate disodium-enhanced magnetic resonance imaging (MRI) shows higher sensitivity for diagnosing hepatocellular carcinoma (HCC), its arterial-phase images may be unsatisfactory because of weak arterial enhancement. We investigated the clinical effectiveness of arterial subtraction images from gadoxetate disodium-enhanced MRI for diagnosing early-stage HCC using the Liver Imaging Reporting and Data System (LI-RADS) v2018.

Methods: In 258 patients at risk of HCC who underwent gadoxetate disodium-enhanced MRI in 2016, a total of 372 hepatic nodules (273 HCCs, 18 other malignancies, and 81 benign nodules) of 3.0 cm or smaller were retrospectively analyzed. Final diagnosis was assessed histopathologically or clinically (marginal recurrence after treatment or change in lesion size on follow-up imaging). The detection rate for arterial hyperenhancement was compared between ordinary arterial-phase and arterial subtraction images, and the benefit of arterial subtraction images in diagnosing HCC using LI-RADS was assessed.

Results: Arterial subtraction images had a significantly higher detection rate for arterial hyperenhancement than ordinary arterial-phase images, both for all hepatic nodules (72.3% vs. 62.4%, $p < 0.001$) and HCCs (91.9% vs. 80.6%, $p < 0.001$). Compared with ordinary arterial-phase images, arterial subtraction images significantly increased the sensitivity of LI-RADS category 5 for diagnosis of HCC (64.1% [173/270] vs. 55.9% [151/270], $p < 0.001$), without significantly decreasing specificity (92.9% [91/98] vs. 94.9% [93/98], $p = 0.155$). For histopathologically confirmed lesions, arterial subtraction images significantly increased sensitivity to 68.8% (128/186) from the 61.3% (114/186) of ordinary arterial-phase images ($p < 0.001$), with a minimal decrease in specificity to 84.8% (39/46) from 89.1% (41/46) ($p = 0.151$).

Conclusions: Arterial subtraction images of gadoxetate disodium-enhanced MRI can significantly improve the sensitivity of early-stage HCC diagnosis using LI-RADS, without a significant decrease in specificity.

Lay summary: Gadoxetate disodium-enhanced magnetic resonance imaging is an imaging technique with a high sensitivity for the diagnosis of hepatocellular carcinoma. However, arterial-phase images may be unsatisfactory because of weak arterial enhancement. We found that using arterial subtraction images led to clinically meaningful improvements in the diagnosis of early-stage hepatocellular carcinoma.

© 2019 European Association for the Study of the Liver. Published by Elsevier B.V. All rights reserved.

Introduction

Hepatocellular carcinoma (HCC) is the most common primary hepatic malignancy and the third most frequent cause of cancer-related deaths.^{1,2} Although the prognosis of patients with advanced HCC remains poor, patients with early-stage HCC are eligible for curative treatments such as surgical resection, local ablation, and liver transplantation.^{3,4} Therefore, accurate imaging diagnosis of early-stage HCC is important.

To standardize the imaging diagnosis of HCC in at-risk patients, the Liver Imaging Reporting and Data System (LI-RADS) was developed in 2011,⁵ updated in 2014, 2017 and 2018, and unified with the American Association for the Study of Liver Disease (AASLD) 2018 HCC clinical practice guidance.⁶ LI-RADS categorizes each hepatic observation according to its likelihood of benignity and HCC (*i.e.*, LR-1 to LR-5). Major features in the LI-RADS v2018 include arterial-phase hyperenhancement, enhancing capsule, non-peripheral washout, and threshold growth. Although all of these major features are significantly associated with HCC, it is of the utmost importance to detect arterial-phase hyperenhancement for the diagnosis of HCC and evaluation of treatment response.^{7–9}

Some early-stage HCCs (17.3–31.6%) may not show arterial-phase hyperenhancement, and this results in a low sensitivity for the diagnosis of HCC.^{10–16} Moreover, as arterial-phase enhancement on gadoxetate disodium (Eovist/Primovist; Bayer HealthCare, Berlin, Germany)-enhanced magnetic resonance imaging (MRI) is weaker than that on extracellular contrast-enhanced MRI, the detection rate for arterial-phase hyperenhancement of early-stage HCCs may be reduced on gadoxetate

Keywords: Hepatocellular carcinoma; Magnetic resonance imaging; Gadoxetate disodium; Subtraction technique; Diagnosis; LI-RADS.

Received 18 December 2018; received in revised form 1 April 2019; accepted 3 May 2019; available online 18 May 2019

* Corresponding author. Address: Department of Radiology and Research Institute of Radiology, University of Ulsan College of Medicine, Asan Medical Center, 88 Olympic-Ro 43-Gil, Songpa-Gu, Seoul 05505, Republic of Korea. Tel.: +82 2 3010 4400, fax: +82 2 476 4719.

E-mail address: jhbyun@amc.seoul.kr (J.H. Byun).

[†] Dong Hwan Kim and Sang Hyun Choi contributed equally to this work as co-first authors.



disodium-enhanced MRI in comparison with extracellular contrast agents.¹⁷ To overcome the weak arterial enhancement of gadoxetate disodium, the LI-RADS v2018 suggests (as a technical recommendation) the use of subtraction images between the unenhanced and arterial phases, which many commercially available MRI systems with recent technical advances in image registration techniques allow.⁶ Although a few previous studies have reported the added value of the arterial subtraction images for diagnosing HCCs on gadoxetate disodium-enhanced liver MRI,^{15,16} the clinical impact of arterial subtraction images on gadoxetate disodium-enhanced MRI has not been investigated using the LI-RADS.

Therefore, the present study aimed to evaluate the clinical impact of arterial subtraction images on gadoxetate disodium-enhanced MRI in the diagnosis of HCCs ≤ 3 cm using the LI-RADS v2018 through the use of a historical cohort study.

Materials and methods

Study population

This study was approved by our institutional review board, and the requirement for informed consent was waived because data

were taken from the clinical cohort of a HCC surveillance program and analyzed retrospectively.⁷ According to the protocol, 3,854 patients at risk of HCC underwent surveillance ultrasound at Asan Medical Center, a 2,700-bed academic tertiary referral hospital in Seoul, in 2016. When a hepatic nodule ≥ 1 cm in diameter was detected on ultrasound, the patient was referred for further evaluations including dynamic computed tomography (CT) or MRI.

From January 2016 to December 2016, 746 patients underwent gadoxetate disodium-enhanced MRI for the evaluation of suspicious nodules detected during ultrasound surveillance (Fig. 1). Patients were included according to the following criteria: (i) focal hepatic solid nodules were observed on MRI; (ii) nodule size was equal to or smaller than 3 cm; (iii) 5 or fewer nodules were observed on MRI;^{10,18} and (iv) the nodule was not definitely or probably benign in imaging studies, *i.e.*, cyst, hemangioma, vascular anomaly, perfusion alternation, hepatic fat deposition or sparing, hypertrophic pseudomass, confluent fibrosis, or focal scar.⁵ Of the 569 available nodules in 396 patients, 184 nodules were excluded because a final diagnosis was absent. This was caused by an insufficient follow-up period of less than 24 months (38 nodules in 18 patients), or immedi-

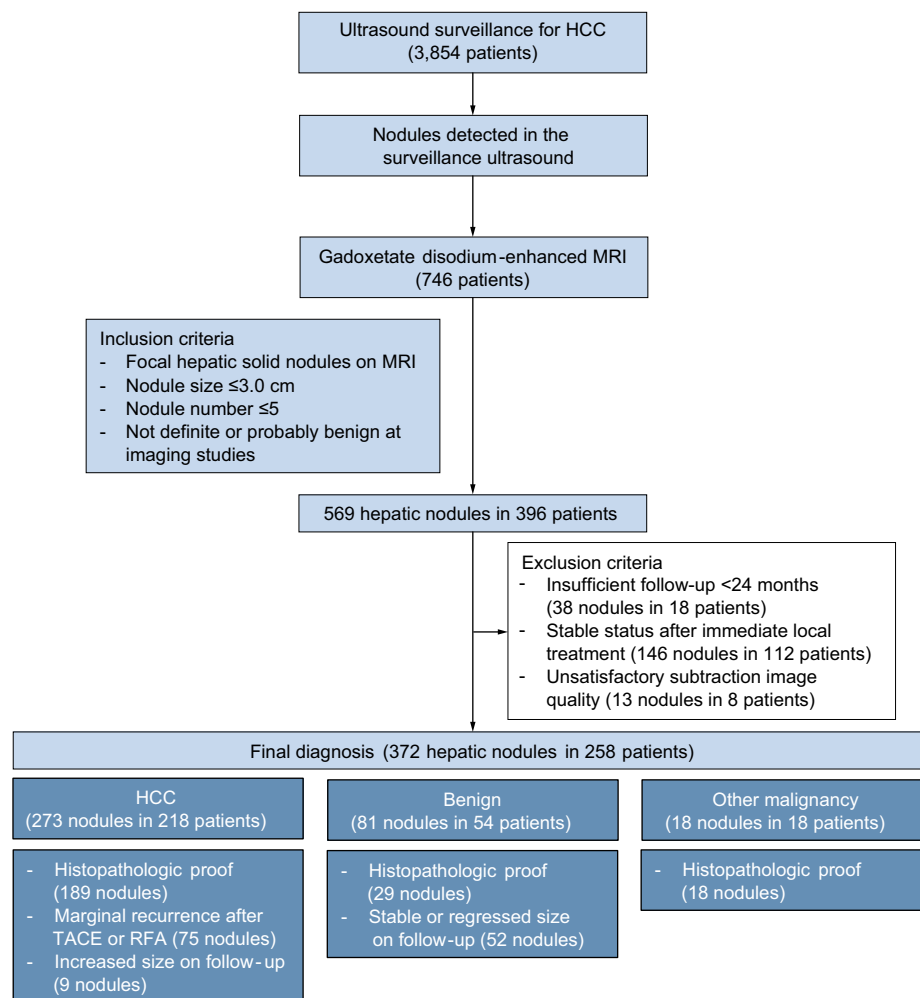


Fig. 1. Flow diagram of subject selection. HCC, hepatocellular carcinoma; MRI, magnetic resonance imaging; RFA, radiofrequency ablation; TACE, transcatheter arterial chemoembolization; US, ultrasonography.

ate loco-regional treatment such as transcatheter arterial chemoembolization (TACE) or radiofrequency ablation (RFA) without biopsy or marginal tumor recurrence (146 nodules in 112 patients). Finally, 385 nodules in 266 patients were used for the analysis.

MR imaging techniques

All patients underwent MRI examinations on a 1.5-T (n = 134; Magnetom Avanto, Siemens Healthcare, Erlangen, Germany) or 3-T scanner (n = 132; Magnetom Skyra, Siemens Healthcare). Unenhanced MRI included T1-weighted dual gradient-echo in- and opposed-phase imaging, T2-weighted navigator-triggered turbo spin-echo imaging, and diffusion-weighted single-shot spin-echo echo-planar imaging. Gadoxetate disodium-enhanced imaging was performed using a bolus injection of 0.025 mmol/kg gadoxetate disodium at a rate of 1.0 ml/s followed by a subsequent 20 ml saline flush delivered using a power injector (Spectris Solaris; Medrad, Warrendale, PA). T1-weighted 3D gradient-echo imaging was obtained before contrast injection, and in the arterial phase (*i.e.*, 5 seconds after peak aortic enhancement determined using a 1 ml test bolus injection), portal venous phase (50 s), transitional phase (3 min), and hepatobiliary phase (HBP; 20 min) of contrast enhancement. Subtraction images were automatically generated after the image acquisition by co-registration software (Inline Liver Registration, Siemens Healthcare) that provided image-by-image subtractions between the unenhanced and arterial phases of each patient. Details of the MRI techniques are given in [Table S1](#).

MR image analysis and LI-RADS category assignment

MR images were anonymized, randomized, and independently reviewed by 2 board-certified abdominal radiologists (each with >7 years of experience in hepatic imaging). The review involved a double blinded reading, *i.e.*, the reviewers were blinded to the pathological results and the other reviewer's results. If any interpretations demonstrated discrepancies between the reviewers, the 2 readers re-evaluated the examinations together and reached a consensus.

On the basis of previous work,¹⁹ one of the reviewers also analyzed the image quality of arterial subtraction images using the following 5-point scale: 1, overall non-diagnostic image quality; 2, severe subtraction artifacts (maximum thickness of subtraction bands >5 mm, or more than two-thirds of either the liver margins or vascular markings are ill defined); 3, moderate subtraction artifacts (maximum thickness of subtraction bands of 2–5 mm, or between one-third and two-thirds of either the liver margins or vascular markings are ill defined); 4, good overall image quality with minimal artifacts (maximum thickness of subtraction bands <2 mm, or less than one-third of either the liver margins or vascular markings are ill defined); and 5, perfect overall image quality without any artifacts. Grades 4 and 5 were regarded as satisfactory image quality for arterial subtraction images. Lesions with unsatisfactory image qualities were excluded from further evaluation.

The reviewers analyzed nodule size, location, and the presence or absence of major features (arterial-phase hyperenhancement, non-peripheral washout, or enhancing capsule), targetoid mass features, and ancillary features, according to the LI-RADS v2018.⁶ Arterial-phase hyperenhancement was defined as non-rim-like enhancement unequivocally greater in

whole or in part than the liver.⁶ If the hyperenhancement was most pronounced in the periphery of the nodule, it was further classified as rim enhancement.⁶ The reviewers evaluated the presence of arterial-phase hyperenhancement using both ordinary arterial-phase images and arterial subtraction images. In the case of T1 hyperintensity, the reviewers determined the presence of arterial-phase hyperenhancement by the qualitative assessment between unenhanced and arterial-phase images. After analyzing the unenhanced, arterial, portal venous, transitional, and HBP images, the reviewers left a 4-week interval before analyzing the arterial subtraction images, to avoid recall bias.

Determination of final diagnosis

Of the 385 nodules in 266 patients, 283 nodules in 225 patients were confirmed as HCC on the basis of pathologic evidence (184 nodules by resection or explantation and 11 by biopsy), marginal recurrence after RFA or TACE (79 nodules), or the growth of the lesion on follow-up imaging over 24 months (9 nodules). Eighty-four nodules in 56 patients were considered benign. A final benign diagnosis was obtained by examination of histopathological specimens (29 nodules including 24 dysplastic nodules, 1 hyalinized nodule, 1 hemangioma, 1 chronic granulomatous inflammation, 1 biliary adenoma, and 1 angiomyolipoma) or a stable or regressed nodule size for at least 24 months (55 nodules).¹⁴ The remaining 18 nodules in 18 patients were pathologically confirmed as other malignancies (17 nodules by resection or explantation and 1 by biopsy), including 11 combined HCC and cholangiocarcinomas (cHCC-CCs), 6 intrahepatic cholangiocarcinomas (IHCCs), and 1 metastatic adenocarcinoma of unknown primary origin. Of the 266 patients, 29 had both HCC (35 nodules) and benign lesion (39 nodules), 3 patients had both HCC (3 nodules) and other malignancy (3 nodules), and 1 patient had both other malignancy (1 nodule) and benign lesion (2 nodules).

Statistical analysis

The detection rates for arterial-phase hyperenhancement on the ordinary arterial-phase images and arterial subtraction images were compared using the McNemar test. Subgroup analysis of the detection rates for arterial-phase hyperenhancement was performed according to the diagnosis (HCCs, other malignancies, or benign lesions), lesion size (≤ 2 cm or > 2 cm), and method of obtaining the final diagnosis (pathological or clinical diagnosis).

To assess the clinical impact of arterial subtraction images for diagnosing early-stage HCC using the LI-RADS v2018, the sensitivity and specificity of the ordinary arterial-phase images and arterial subtraction images were analyzed and then compared using the McNemar test.

Interobserver agreement for arterial hyperenhancement on the ordinary arterial-phase images, arterial hyperenhancement on the arterial subtraction images, washout during the portal venous phase, and enhancing capsule was evaluated using the overall percentage of agreement and the weighted κ statistic.²⁰ In the per-lesion analysis, generalized estimating equations were used to adjust for the correlations between multiple nodules within a single patient (*i.e.*, a clustering effect).²¹ A *p* value of <0.05 was considered statistically significant. Statistical analysis was performed using SAS v 9.4 (SAS Institute, Cary, NC).

Results

The quality of arterial subtraction images

Of the 266 patients, 8 patients showed a misregistration artifact (grade 2, 4 patients; grade 3, 4 patients) that resulted in unsatisfactory image quality and were excluded from further evaluation.

Patient characteristics

After excluding the 8 patients with unsatisfactory image quality, we finally analyzed 258 patients with 372 hepatic nodules (273 HCCs, 6 IHCCs, 11 cHCC-CCs, 1 metastasis, and 81 benign lesions). The clinical and MRI characteristics of the 372 nodules in 258 patients are summarized in Table 1 and Table S2. There

were 210 men (81.4%) and 48 women (18.6%), with a mean age of 61 years (range, 33–84). Hepatitis B was the predominant cause of chronic liver disease (n = 204, 79.1%), followed by alcohol-related liver disease (n = 24, 9.3%). The size of the 372 nodules ranged from 5 mm to 30 mm (mean size, 18.4 mm).

Detection rate for arterial-phase hyperenhancement

For the hepatic nodules as a whole, arterial subtraction images had a significantly higher detection rate for arterial-phase hyperenhancement than the ordinary arterial-phase images (72.3% [269/372] vs. 62.4% [232/372]; *p* <0.001; Table 2). In the subgroup analyses, arterial subtraction images showed higher rates of arterial-phase hyperenhancement than ordinary arterial-phase images, for both HCCs (91.9% [251/273] vs. 80.6% [220/273]; *p* <0.001; Figs. 2 and 3) and other malignancies (72.2% [13/18] vs. 44.4% [8/18]; *p* = 0.025). For benign lesions, the detection rate for arterial-phase hyperenhancement was not significantly different between the 2 images (*p* = 0.317). Arterial subtraction images detected arterial-phase hyperenhancement significantly better than ordinary arterial-phase images, both in nodules less than or equal to 2 cm in diameter (61.9% [143/231] vs. 52.0% [120/231]; *p* <0.001; Fig. 2) and in nodules greater than 2 cm in diameter (89.4% [126/141] vs. 79.4% [112/141]; *p* <0.001; Fig. 3). Arterial subtraction images also demonstrated arterial hyperenhancement significantly better than ordinary arterial-phase images in both pathologically confirmed lesions and lesions with a clinical diagnosis (*p* <0.001).

Interobserver agreement for arterial hyperenhancement on arterial subtraction images (overall percentage of agreement, 93.8%; κ , 0.889) was better than that on the ordinary arterial-phase images (overall percentage of agreement, 86.9%; κ , 0.723; Table S3). For the washout appearance and enhancing capsule, the overall percentages of agreement were 82.0% (κ , 0.635) and 82.5% (κ , 0.582), respectively (Table S3).

Diagnostic accuracy for HCC using the LI-RADS

Using the ordinary arterial-phase images, the final LI-RADS categories of 372 nodules included LR-3 (intermediate probability of malignancy) in 19 nodules, LR-4 (probably HCC) in 174 nodules, LR-5 (definitely HCC) in 156 nodules, LR-M (probably or definitely malignant, not HCC specific) in 19 nodules, and LR-TIV (malignancy with tumor in vein) in 4 nodules. Using the arterial subtraction images, the final LI-RADS categories of 372

Table 1. Clinical characteristics of the 258 patients.

Characteristics	Total (n = 258)
Mean age (range) (years)	61 (33–84)
Sex, male:female	210:48
No. of nodules	
1	178 (69.0)
2	55 (21.2)
3	19 (7.4)
4	3 (1.2)
5	3 (1.2)
Risk factors	
Hepatitis B	204 (79.1)
Hepatitis C	12 (4.7)
Hepatitis B and C	2 (0.8)
Alcohol-related liver disease	24 (9.3)
Others [†]	16 (6.1)
Child-Pugh classification [‡]	
A	233 (90.7)
B	20 (7.8)
C	4 (1.5)
LI-RADS category [‡]	
LR-3	19 (5.1)
LR-4	174 (46.8)
LR-5	156 (41.9)
LR-M	19 (5.1)
LR-TIV	4 (1.1)
Tumor marker	
Median AFP (range) (ng/ml)	7.3 (0.1–111,953)

Data are number (%) of patients.

LI-RADS, Liver Imaging Reporting and Data System; AFP, alpha-fetoprotein.

[†]Others included liver cirrhosis caused by non-alcoholic fatty liver disease (n = 3) and cryptogenic liver cirrhosis (n = 13).

[‡]One patient had no available information.

[§]Data are number (%) of nodules. The total number of nodules is 372.

Table 2. The detection rates for arterial hyperenhancement on ordinary arterial-phase images and arterial subtraction images for all 372 nodules from 258 patients.

	Ordinary arterial-phase images	Arterial subtraction images	<i>p</i>
Total (n = 372)	232 (62.4)	269 (72.3)	<0.001
Diagnosis			
HCC (n = 273)	220 (80.6)	251 (91.9)	<0.001
Other malignancies (n = 18)	8 (44.4)	13 (72.2)	0.025
Benign lesion (n = 81)	4 (4.9)	5 (6.2)	0.317
Size of nodule			
≤2 cm (n = 231)	120 (52.0)	143 (61.9)	<0.001
>2 cm (n = 141)	112 (79.4)	126 (89.4)	<0.001
Diagnostic method			
Histopathology (n = 236)	170 (72.0)	192 (81.4)	<0.001
Clinical diagnosis (n = 136) [†]	62 (45.6)	77 (56.6)	<0.001

Data are number (%) of nodules.

HCC, hepatocellular carcinoma.

[†]Marginal tumor recurrence after transcatheter arterial chemoembolization or radiofrequency ablation, growth of the lesion on follow-up imaging studies, or stable or regressed nodule size for at least 24 months.

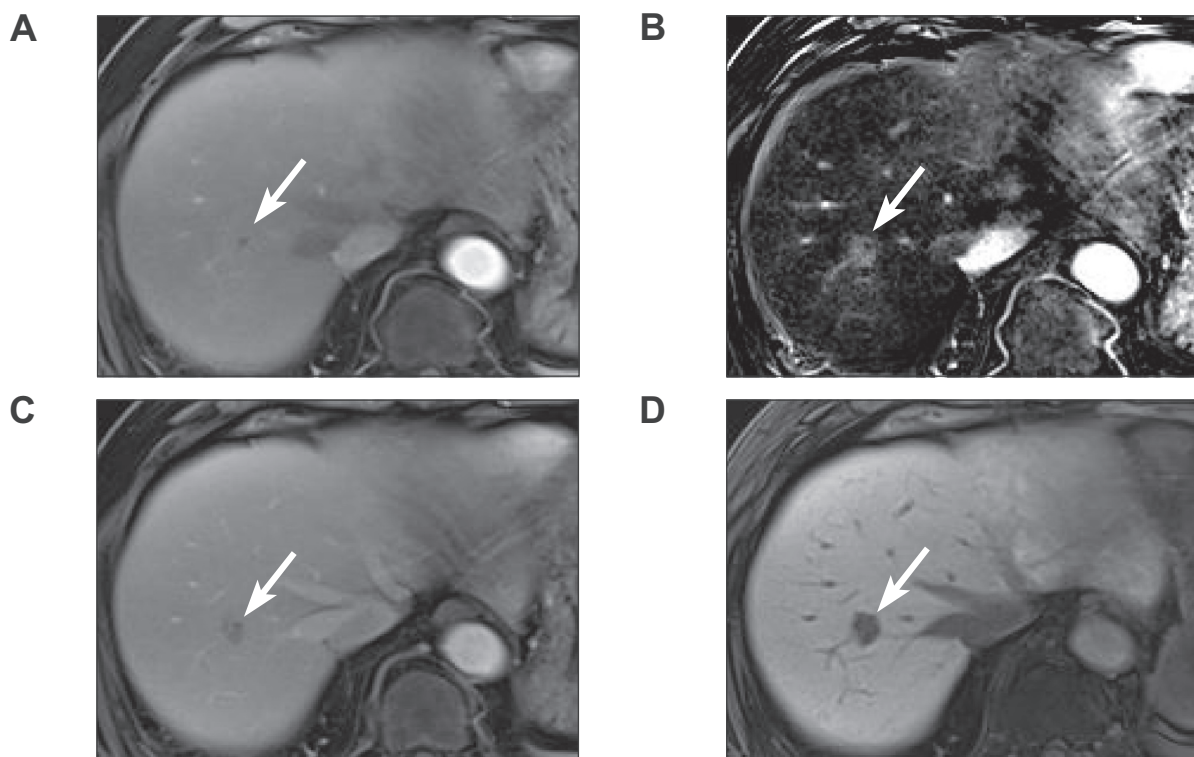


Fig. 2. A 62-year-old man with chronic hepatitis B and surgically confirmed hepatocellular carcinoma. (A) The ordinary arterial-phase image of gadopentate disodium-enhanced MRI does not depict arterial hyperenhancement, whereas (B) the arterial subtraction image shows hyperenhancement of a 1.6 cm nodule (arrow) in hepatic segment VIII. The nodule (arrow) has a washout appearance (C) on the portal venous phase image and shows hypointensity (D) on the hepatobiliary phase image. The lesion was classified as LI-RADS category 4 on the basis of ordinary arterial-phase images, whereas this category was changed to LI-RADS category 5 when arterial subtraction images were used. The arterial subtraction images enabled us to make a diagnosis of HCC in this patient. HCC, hepatocellular carcinoma, LI-RADS, Liver Imaging Reporting and Data System.

nodules included LR-3 in 18 nodules, LR-4 in 154 nodules, LR-5 in 180 nodules, LR-M in 16 nodules, and LR-TIV in 4 nodules. After excluding 4 LR-TIV nodules,⁶ we included 254 patients with 368 hepatic nodules in the following analysis.

When LR-5 was regarded as HCC, ordinary arterial-phase images showed a sensitivity of 55.9% (151/270) and a specificity of 94.9% (93/98) for the diagnosis of HCC (Table 3). When we determined arterial-phase hyperenhancement on the arterial subtraction images, the sensitivity showed a statistically significant increase to 64.1% (173/270; $p < 0.001$), whereas the specificity decreased to 92.9% (91/98), but this decrease was not statistically significant ($p = 0.155$). In comparison with the ordinary arterial-phase images, the arterial subtraction images detected 22 additional HCCs (Figs. 2 and 3) at a cost of only 2 additional false-positive diagnoses (Fig. 4). These 2 false-positive nodules included 1 IHCC and 1 cHCC-CC, both of which showed iso- or hypointensity on ordinary arterial-phase images, but hyperenhancement on arterial subtraction images (Fig. 4). When both LR-4 and LR-5 were regarded as HCC, the differences in sensitivity and specificity between the ordinary arterial-phase images and arterial subtraction images were not significantly different ($p = 0.082$ and 0.297 , respectively; Table 3).

In the subgroup analysis of pathologically confirmed lesions (186 HCCs and 46 non-HCCs), the sensitivity and specificity for the diagnosis of HCC showed similar trends to those of the whole study group (Table 4). When LR-5 was regarded as HCC, arterial subtraction images significantly increased the sensitivity to 68.8% (128/186) from the 61.3% (114/186) on the ordinary arterial-phase images ($p < 0.001$), with a minimal

decrease in specificity to 84.8% (39/46) from 89.1% (41/46) ($p = 0.151$). When both LR-4 and LR-5 were regarded as HCC, the differences in sensitivity and specificity between ordinary arterial-phase images and arterial subtraction images were not significantly different ($p = 0.082$ and 0.285 , respectively; Table 4).

Discordant arterial hyperenhancement between arterial subtraction images and ordinary arterial-phase images

In the detection of arterial-phase hyperenhancement, 335 (90.1%) nodules showed consistency between the ordinary arterial-phase images and arterial subtraction images: 232 nodules showed arterial-phase hyperenhancement on both the images, whereas 103 nodules showed no arterial-phase hyperenhancement.

Of the 37 (9.9%) nodules showing an inconsistency between the 2 images (Table 5), 33 nodules showed iso- or hypointensity on the ordinary arterial-phase images, but hyperenhancement on the arterial subtraction images. The final diagnoses of these 33 nodules were 29 HCCs (87.9%; 29/33), 2 IHCCs, 1 cHCC-CC, and 1 benign lesion. The remaining 4 inconsistent nodules showed rim enhancement on the ordinary arterial-phase images, but hyperenhancement on the arterial subtraction images. The final diagnoses of these 4 nodules were 2 HCCs, 1 IHCC, and 1 cHCC-CC.

Twenty-three (62.1%) nodules were equal to or smaller than 2 cm in diameter, and 14 (37.9%) nodules were larger than 2 cm. After using the arterial subtraction images, the LI-RADS categories for 26 nodules were changed as follows: 1 LR-3 nodule

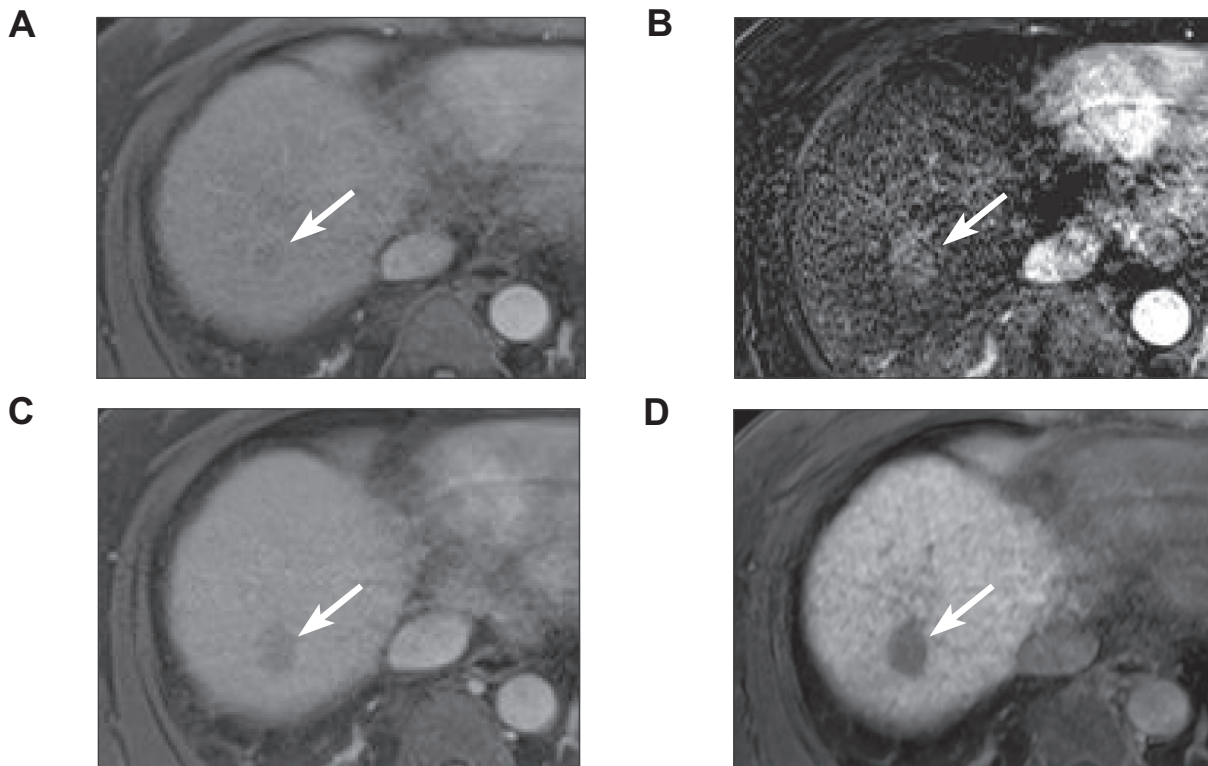


Fig. 3. A 54-year-old man with chronic hepatitis B and surgically confirmed hepatocellular carcinoma. (A) The ordinary arterial-phase image of gadoxetate disodium-enhanced MRI does not depict arterial hyperenhancement, whereas (B) the arterial subtraction image shows hyperenhancement of a 2.2 cm nodule (arrow) in hepatic segment VIII. The nodule (arrow) has a washout appearance (C) on the portal venous phase image and shows hypointensity (D) on the hepatobiliary phase image. The lesion was classified as LI-RADS category 4 on the basis of ordinary arterial-phase images, whereas this category was changed to LI-RADS category 5 when arterial subtraction images were used. LI-RADS, Liver Imaging Reporting and Data System.

Table 3. Comparison of ordinary arterial-phase and arterial subtraction images in the diagnosis of HCC in 368 hepatic nodules according to the LI-RADS.

LI-RADS category	True-positive	False-negative	False-positive	True-negative	Sensitivity, %	<i>p</i>	Specificity, %	<i>p</i>
LR-5								
Ordinary arterial-phase images	151	119	5	93	55.9 (49.8–61.9)	<0.001*	94.9 (88.1–97.9)	0.155†
Arterial subtraction images	173	97	7	91	64.1 (57.9–69.9)		92.9 (85.5–96.6)	
LR-4 and LR-5								
Ordinary arterial-phase images	254	16	76	22	94.1 (90.6–96.3)	0.082‡	22.4 (14.5–33.0)	0.297§
Arterial subtraction images	257	13	77	21	95.2 (91.9–97.2)		21.4 (13.9–31.6)	

After excluding 4 LR-TIV nodules from the entire group of 372 nodules, 368 hepatic nodules were used for the analysis. Data are the number of nodules. Numbers in parentheses are 95% confidence intervals.

HCC, hepatocellular carcinoma; LI-RADS, Liver Imaging Reporting and Data System; TIV, tumor in vein.

*Comparison of sensitivity between ordinary arterial-phase image and arterial subtraction image when LR-5 was diagnosed as HCC.

†Comparison of specificity between ordinary arterial-phase image and arterial subtraction image when LR-5 was diagnosed as HCC.

‡Comparison of sensitivity between ordinary arterial-phase image and arterial subtraction image when both LR-4 and LR-5 were diagnosed as HCC.

§Comparison of specificity between ordinary arterial-phase image and arterial subtraction image when both LR-4 and LR-5 were diagnosed as HCC.

was changed to LR-4, 22 LR-4 nodules were changed to LR-5, and 3 LR-M nodules were changed to LR-4 or LR-5. All of the 22 nodules changed from LR-4 to LR-5 showed non-peripheral washout.

Discussion

This study demonstrated that, on gadoxetate disodium-enhanced MRI, arterial subtraction images had a significantly higher detection rate for arterial-phase hyperenhancement than ordinary arterial-phase images. The arterial subtraction images also resulted in higher interobserver agreement than the ordinary arterial-phase images. In addition, the use of arterial

subtraction images significantly increased the sensitivity of the LR-5 category in the LI-RADS v2018 for diagnosis of early-stage HCC (64.1% [173/270] vs. 55.9% [151/270], $p < 0.001$), without significantly decreasing the specificity (92.9% [91/98] vs. 94.9% [93/98], $p = 0.155$).

Arterial-phase hyperenhancement is one of the most important imaging features for diagnosing HCC in the LI-RADS v2018.⁶ As arterial-phase hyperenhancement results from neoangiogenesis of the unpaired artery in the nodule during hepatocarcinogenesis^{22,23} and 68.4–82.7% of early-stage HCCs show arterial-phase hyperenhancement,^{10–16} the detection of arterial-phase hyperenhancement is very important for the diagnosis of HCC. Although gadoxetate disodium-enhanced

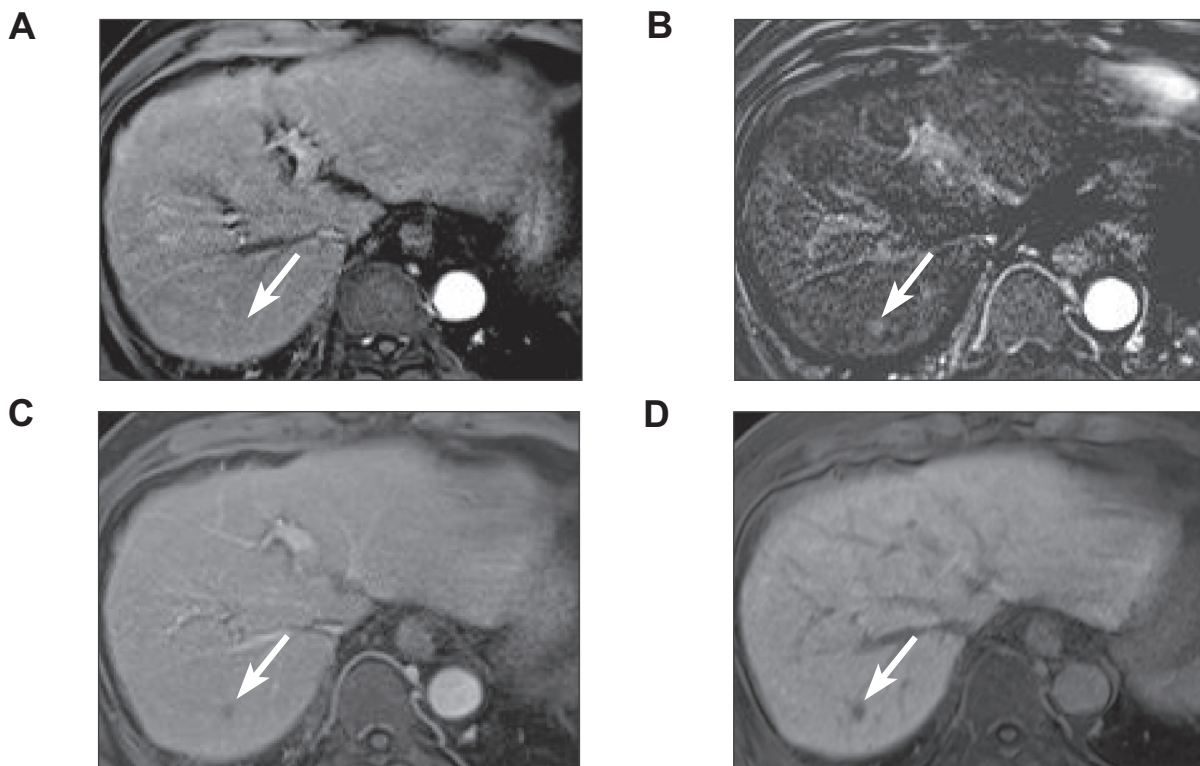


Fig. 4. A 69-year-old man with chronic hepatitis B and surgically confirmed cholangiocarcinoma. (A) The ordinary arterial-phase image of gadoxetate disodium-enhanced MRI does not show arterial hyperenhancement, whereas (B) the arterial subtraction image shows hyperenhancement of a 1.2 cm nodule (arrow) in hepatic segment VII. The nodule (arrow) has a washout appearance (C) on the portal venous phase image and shows hypointensity (D) on the hepatobiliary phase image. The LI-RADS category of the nodule was changed from LR-4 to LR-5 when arterial subtraction images were used. This case was 1 of 2 additional false-positive results that occurred after using the arterial subtraction images. LI-RADS, Liver Imaging Reporting and Data System.

Table 4. Comparison of ordinary arterial-phase and arterial subtraction images in the diagnosis of HCC according to the LI-RADS in the subgroup of 232 histopathologically confirmed nodules.

LI-RADS category	True-positive	False-negative	False-positive	True-negative	Sensitivity, %	<i>p</i>	Specificity, %	<i>p</i>
LR-5								
Ordinary arterial-phase images	114	72	5	41	61.3 (54.1–68.1)	<0.001 [*]	89.1 (75.8–95.5)	0.151 [†]
Arterial subtraction images	128	58	7	39	68.8 (61.9–75.0)		84.8 (70.5–92.8)	
LR-4 and LR-5								
Ordinary arterial-phase images	174	12	31	15	93.5 (89.0–96.3)	0.082 [‡]	32.6 (19.7–48.9)	0.285 [§]
Arterial subtraction images	177	9	32	14	95.2 (91.0–97.5)		30.4 (18.3–46.1)	

After excluding 4 LR-TIV nodules and 136 nodules with a clinical diagnosis, 232 hepatic nodules were used in this analysis. Data are the number of nodules. Numbers in parentheses are 95% confidence intervals.

HCC, hepatocellular carcinoma; LI-RADS, Liver Imaging Reporting and Data System; TIV, tumor in vein.

^{*}Comparison of sensitivity between ordinary arterial-phase image and arterial subtraction image when LR-5 was diagnosed as HCC.

[†]Comparison of specificity between ordinary arterial-phase image and arterial subtraction image when LR-5 was diagnosed as HCC.

[‡]Comparison of sensitivity between ordinary arterial-phase image and arterial subtraction image when both LR-4 and LR-5 were diagnosed as HCC.

[§]Comparison of specificity between ordinary arterial-phase image and arterial subtraction image when both LR-4 and LR-5 were diagnosed as HCC.

MRI shows higher sensitivity for diagnosing HCC,^{24–27} its arterial-phase images may be unsatisfactory because of weak arterial enhancement.^{6,7,28} To overcome this weakness, various methods have been investigated, including modification of injection protocols, optimization of arterial-phase scan timing, and optimization of image acquisition.²⁸ In the present study, arterial subtraction images significantly increased the detection rate for arterial-phase hyperenhancement (72.3% [269/372] vs. 62.4% [232/372], *p* <0.001) in comparison with ordinary arterial-phase images. This result is similar to the findings of previous studies that reported an increased detection rate for arterial-phase hyperenhancement using arterial subtraction images, *i.e.*, from 59.3–72.4% to 64.4–89.2%.^{15,16} As arterial subtraction images can detect more arterial-phase hyperenhance-

ment and can be easily obtained using commercially available software without an additional image acquisition, we consider arterial subtraction images to be clinically useful in the diagnosis of HCC.

The LR-5 category has a high specificity for the diagnosis of HCC;^{29–31} it is essentially equivalent to the Organ Procurement and Transplantation Network class 5 with one exception, and can be used to avoid misdiagnosis of HCC in liver transplant candidates.^{31,32} This explains the low sensitivity of LR-5 for the diagnosis of HCC. In the present study, the sensitivity of LR-5 was 55.9% (151/270), which was similar to the values reported in recent studies (42.3–50.8%).^{29–31} However, given that patients with early-stage HCC are eligible for curative treatments such as surgical resection, liver transplantation, and

Table 5. Characteristics of the 37 nodules with discordant arterial hyperenhancement between ordinary arterial-phase images and arterial subtraction images.

Characteristics	Total (n = 37)
Ordinary arterial-phase images	
Iso- or hypointensity	33
Rim enhancement	4
Diagnosis	
Histopathological (n = 22)	
HCC	17
Cholangiocarcinoma	3
Combined HCC and cholangiocarcinoma	2
Clinical (n = 15)	
HCC	14
Benign lesion	1
Grade of histopathologically confirmed HCC (n = 17)	
Edmondson-Steiner grade 2	6
Edmondson-Steiner grade 3	9
Edmondson-Steiner grade 4	2
Mean size (range) (mm)	18.4 (7–30)
<10 mm	6 (16.2)
10–20 mm	17 (45.9)
>20 mm	14 (37.9)
Change of LI-RADS category [†]	
LR-3 to LR-4	1 (2.7)
LR-4 to LR-5	22 (59.5)
LR-M to LR-4	1 (2.7)
LR-M to LR-5	2 (5.4)
Not changed	11 (29.7)

Data are number (%) of nodules except for mean size.

HCC, hepatocellular carcinoma; LI-RADS, Liver Imaging Reporting and Data System.

[†]Lesions seen as iso- or hypointensity or rim enhancement on ordinary arterial-phase images and hyperenhancement on arterial subtraction images.

[‡]Change in LI-RADS category when arterial subtraction images were used.

RFA,^{1,3,4,33} it is important to improve this sensitivity. This study found that arterial subtraction images significantly increased the sensitivity of LR-5 from 55.9% (151/270) to 64.1% (173/270; $p < 0.001$), without a significant difference in specificity (94.9% [93/98] vs. 92.9% [91/98], $p = 0.155$). In this regard, the arterial subtraction images suggested in the technical recommendation can be useful when applying the LI-RADS v2018, and might be an option for increasing the sensitivity of LR-5 for diagnosing early-stage HCC, especially on gadoxetate disodium-enhanced MRI.

Of the 37 discordant nodules between the ordinary arterial-phase images and arterial subtraction images, 83.8% (31/37) were HCCs and 16.2% (6/37) were non-HCCs. Using arterial subtraction images, arterial-phase hyperenhancement was additionally detected in all 31 of the HCCs, with 22 of these 31 HCCs being further correctly classified into LR-5. The 6 non-HCC nodules included 3 IHCCs, 2 cHCC-CCs, and 1 benign lesion. Although arterial-phase hyperenhancement was additionally detected on arterial subtraction images in these 6 non-HCC nodules, the LI-RADS category was changed in only 3 nodules: 2 nodules (1 IHCC and 1 cHCC-CC) were changed from LR-4 to LR-5, and 1 (cHCC-CC) from LR-M to LR-4. Finally, of these 3 nodules, the 2 that were changed from LR-4 to LR-5 after use of the arterial subtraction images resulted in 2 additional false-positives. In daily practice, accurate discrimination between HCC and other malignancies on diagnostic imaging might occasionally be difficult in the setting of cirrhosis or chronic liver disease, because substantial proportions of IHCCs or cHCC-CCs do not show a typical targetoid appearance, partic-

ularly rim arterial hyperenhancement, and may be categorized as LR-4 or LR-5 rather than LR-M.^{34–37}

This study has several limitations. First, the present study may have a selection bias due to its retrospective nature, although we tried our best to minimize this limitation by including a large number of study participants and the use of a historical cohort study design most similar to a real clinical situation. Second, misregistration artifacts on the arterial subtraction images may be another limitation of our analysis. However, most of the artifacts can be overcome with commercially available MRI software, and recent studies have shown that only a small fraction of patients have subtraction images of insufficient quality (2.6–4%).^{15,16} In the present study, only 8 patients (3.0%) were excluded from the study because of degraded image quality due to misregistration artifact. Furthermore, in daily practice we can use the ordinary arterial-phase image in cases where the arterial subtraction images are of insufficient quality. Therefore, this limitation may be not significant. Third, 88 nodules were clinically diagnosed as HCC on the basis of marginal tumor recurrence after TACE or RFA, or interval growth of the lesion on follow-up imaging studies, without obtaining histopathological evidence. However, we followed the AASLD practice guidance, which states that the diagnosis of HCC can be established, and treatment rendered, based on typical imaging features of HCC at multiphase CT or MRI without biopsy confirmation.⁷

In conclusion, detection of the arterial-phase hyperenhancement of early-stage HCCs on gadoxetate disodium-enhanced MRI can be significantly improved by using arterial subtraction images in comparison with the ordinary arterial-phase images. When applied to LI-RADS for diagnosing early-stage HCC, the arterial subtraction images can significantly enhance sensitivity, without a significant decrease in specificity.

Financial support

There was no funding or support from industry for this study.

Conflict of interest

No conflicting relationship exists for any of the authors except for YS Lim. YS Lim is an advisory board member of Bayer Schering Healthcare and Gilead Science, and receives research funding from Bayer Healthcare and Gilead Science.

Please refer to the accompanying ICMJE disclosure forms for further details.

Authors' contributions

SH Choi and JH Byun contributed to study concept and design. SH Choi, DH Kim and JH Kang acquired the data. DH Kim and JH Kang analyzed and interpreted the data. DH Kim and SH Choi drafted the manuscript. DH Kim and SH Choi performed statistical analysis. JH Byun, YS Lim, SJ Lee, SY Kim, HJ Won, YM Shin, and PN Kim made critical revisions to the manuscript. JH Byun supervised the study.

Supplementary data

Supplementary data to this article can be found online at <https://doi.org/10.1016/j.jhep.2019.05.005>.

References

Author names in bold designate shared co-first authorship

- [1] El-Serag HB. Hepatocellular carcinoma. *N Engl J Med* 2011;365:1118–1127.
- [2] El-Serag HB, Rudolph KL. Hepatocellular carcinoma: epidemiology and molecular carcinogenesis. *Gastroenterology* 2007;132:2557–2576.
- [3] Lu DS, Yu NC, Raman SS, Limanond P, Lassman C, Murray K, et al. Radiofrequency ablation of hepatocellular carcinoma: treatment success as defined by histologic examination of the explanted liver. *Radiology* 2005;234:954–960.
- [4] Llovet JM, Fuster J, Bruix J. The Barcelona approach: diagnosis, staging, and treatment of hepatocellular carcinoma. *Liver Transpl* 2004;10: S115–S120.
- [5] Mitchell DG, Bruix J, Sherman M, Sirlin CB. LI-RADS (Liver Imaging Reporting and Data System): summary, discussion, and consensus of the LI-RADS Management Working Group and future directions. *Hepatology* 2015;61:1056–1065.
- [6] American College of Radiology. CT/MRI LI-RADS v2018 core. <https://www.acr.org/-/media/ACR/Files/RADS/LI-RADS/LI-RADS-2018-Core.pdf?la=en>. Accessed December 4, 2018.
- [7] Marrero JA, Kulik LM, Sirlin C, Zhu AX, Finn RS, Abecassis MM, et al. Diagnosis, Staging and Management of Hepatocellular Carcinoma: 2018 Practice Guidance by the American Association for the Study of Liver Diseases. *Hepatology* 2018;68:723–750.
- [8] EASL Clinical Practice Guidelines. Management of hepatocellular carcinoma. *J Hepatol* 2018;69:182–236.
- [9] Lencioni R, Llovet JM. Modified RECIST (mRECIST) assessment for hepatocellular carcinoma. *Semin Liver Dis* 2010;30:52–60.
- [10] Kwon HJ, Byun JH, Kim JY, Hong GS, Won HJ, Shin YM, et al. Differentiation of small ($\leq 2\text{ cm}$) hepatocellular carcinomas from small benign nodules in cirrhotic liver on gadoxetic acid-enhanced and diffusion-weighted magnetic resonance images. *Abdom Imaging* 2015;40:64–75.
- [11] Park MJ, Kim YK, Lee MH, Lee JH. Validation of diagnostic criteria using gadoxetic acid-enhanced and diffusion-weighted MR imaging for small hepatocellular carcinoma ($\leq 2.0\text{ cm}$) in patients with hepatitis-induced liver cirrhosis. *Acta Radiol* 2013;54:127–136.
- [12] Yu MH, Kim JH, Yoon JH, Kim HC, Chung JW, Han JK, et al. Small ($\leq 1\text{-cm}$) hepatocellular carcinoma: diagnostic performance and imaging features at gadoxetic acid-enhanced MR imaging. *Radiology* 2014;271:748–760.
- [13] Kim TK, Lee KH, Jang HJ, Haider MA, Jacks LM, Menezes RJ, et al. Analysis of gadobenate dimeglumine-enhanced MR findings for characterizing small (1–2-cm) hepatic nodules in patients at high risk for hepatocellular carcinoma. *Radiology* 2011;259:730–738.
- [14] Khalili K, Kim TK, Jang HJ, Haider MA, Khan L, Guindi M, et al. Optimization of imaging diagnosis of 1–2 cm hepatocellular carcinoma: an analysis of diagnostic performance and resource utilization. *J Hepatol* 2011;54:723–728.
- [15] An C, Park MS, Kim D, Kim YE, Chung WS, Rhee H, et al. Added value of subtraction imaging in detecting arterial enhancement in small (<math>< 3\text{ cm}</math>) hepatic nodules on dynamic contrast-enhanced MRI in patients at high risk of hepatocellular carcinoma. *Eur Radiol* 2013;23:924–930.
- [16] Choi SH, Kim SY, Lee SS, Shim JH, Byun JH, Baek S, et al. Subtraction images of gadoxetic acid-enhanced MRI: effect on the diagnostic performance for focal hepatic lesions in patients at risk for hepatocellular carcinoma. *AJR Am J Roentgenol* 2017;209:584–591.
- [17] Tirkes T, Mehta P, Aisen AM, Lall C, Akisik F. Comparison of dynamic phase enhancement of hepatocellular carcinoma using gadoxetate disodium vs gadobenate dimeglumine. *J Comput Assist Tomogr* 2015;39:479–482.
- [18] **Piana G, Trinquart L**, Meskine N, Barrau V, Beers BV, Vilgrain V. New MR imaging criteria with a diffusion-weighted sequence for the diagnosis of hepatocellular carcinoma in chronic liver diseases. *J Hepatol* 2011;55:126–132.
- [19] Sundarakumar DK, Wilson GJ, Osman SF, Zaidi SF, Maki JH. Evaluation of image registration in subtracted 3D dynamic contrast-enhanced MRI of treated hepatocellular carcinoma. *AJR Am J Roentgenol* 2015;204:287–296.
- [20] Kundel HL, Polansky M. Measurement of observer agreement. *Radiology* 2003;228:303–308.
- [21] Bland JM. Cluster randomised trials in the medical literature: two bibliometric surveys. *BMC Med Res Methodol* 2004;4:21.
- [22] Hayashi M, Matsui O, Ueda K, Kawamori Y, Kadoya M, Yoshikawa J, et al. Correlation between the blood supply and grade of malignancy of hepatocellular nodules associated with liver cirrhosis: evaluation by CT during intraarterial injection of contrast medium. *AJR Am J Roentgenol* 1999;172:969–976.
- [23] Fournier LS, Cuenod CA, de Bazelaire C, Siauve N, Rosty C, Tran PL, et al. Early modifications of hepatic perfusion measured by functional CT in a rat model of hepatocellular carcinoma using a blood pool contrast agent. *Eur Radiol* 2004;14:2125–2133.
- [24] Choi SH, Byun JH, Lim YS, Yu E, Lee SJ, Kim SY, et al. Diagnostic criteria for hepatocellular carcinoma $\leq 3\text{ cm}$ with hepatocyte-specific contrast-enhanced magnetic resonance imaging. *J Hepatol* 2016;64:1099–1107.
- [25] Lee YJ, Lee JM, Lee JS, Lee HY, Park BH, Kim YH, et al. Hepatocellular carcinoma: diagnostic performance of multidetector CT and MR imaging—a systematic review and meta-analysis. *Radiology* 2015;275:97–109.
- [26] Duncan JK, Ma N, Vreugdenburg TD, Cameron AL, Maddern G. Gadoxetic acid-enhanced MRI for the characterization of hepatocellular carcinoma: a systematic review and meta-analysis. *J Magn Reson Imaging* 2017;45:281–290.
- [27] **Liu X, Jiang H, Chen J**, Zhou Y, Huang Z, Song B. Gadoxetic acid disodium-enhanced magnetic resonance imaging outperformed multi-detector computed tomography in diagnosing small hepatocellular carcinoma: a meta-analysis. *Liver Transpl* 2017;23:1505–1518.
- [28] Huh J, Kim SY, Yeh BM, Lee SS, Kim KW, Wu EH, et al. Troubleshooting arterial-phase MR images of gadoxetate disodium-enhanced liver. *Korean J Radiol* 2015;16:1207–1215.
- [29] Choi SH, Byun JH, Kim SY, Lee SJ, Won HJ, Shin YM, et al. Liver imaging reporting and data system v2014 With gadoxetate disodium-enhanced magnetic resonance imaging: validation of LI-RADS category 4 and 5 criteria. *Invest Radiol* 2016;51:483–490.
- [30] Darnell A, Forner A, Rimola J, Reig M, Garcia-Criado A, Ayuso C, et al. Liver imaging reporting and data system with MR imaging: evaluation in nodules 20 mm or smaller detected in cirrhosis at screening US. *Radiology* 2015;275:698–707.
- [31] Cerny M, Bergeron C, Billiard JS, Murphy-Lavallee J, Olivie D, Berube J, et al. LI-RADS for MR imaging diagnosis of hepatocellular carcinoma: performance of major and ancillary features. *Radiology* 2018;288:118–128.
- [32] Yacoub JH, Miller FH. Understanding LI-RADS, its relationship to AASLD and OPTN, and the challenges of its adoption. *Curr Hepatol Rep* 2017;16:72–80.
- [33] Singal AG, Pillai A, Tiro J. Early detection, curative treatment, and survival rates for hepatocellular carcinoma surveillance in patients with cirrhosis: a meta-analysis. *PLoS Med* 2014;11 e1001624.
- [34] Huang B, Wu L, Lu XY, Xu F, Liu CF, Shen WF, et al. Small intrahepatic cholangiocarcinoma and hepatocellular carcinoma in cirrhotic livers may share similar enhancement patterns at multiphase dynamic MR imaging. *Radiology* 2016;281:150–157.
- [35] An C, Park S, Chung YE, Kim DY, Kim SS, Kim MJ, et al. Curative resection of single primary hepatic malignancy: liver imaging reporting and data system category LR-M portends a worse prognosis. *AJR Am J Roentgenol* 2017;209:576–583.
- [36] Park SH, Lee SS, Yu E, Kang HJ, Park Y, Kim SY, et al. Combined hepatocellular-cholangiocarcinoma: Gadoxetic acid-enhanced MRI findings correlated with pathologic features and prognosis. *J Magn Reson Imaging* 2017;46:267–280.
- [37] Jeon SK, Joo I, Lee DH, Lee SM, Kang HJ, Lee KB, et al. Combined hepatocellular cholangiocarcinoma: LI-RADS v2017 categorisation for differential diagnosis and prognostication on gadoxetic acid-enhanced MR imaging. *Eur Radiol* 2019;29:373–382.